# Local All-Pass Geometric Deformations - Supplementary Material

Christopher Gilliam and Thierry Blu

CONTENTS



C. Gilliam and T. Blu are with the Department of Electronic Engineering, The Chinese University of Hong Kong, Shatin, N.T., Hong Kong. E-mail: {cgilliam, tblu}@ee.cuhk.edu.hk.

This document contains supplementary material for the paper "Local All-Pass Geometric Deformations" by C. Gilliam and T. Blu.

## I. Continuous Description of the Spaghetti Images

The spaghetti images described in the main paper comprise a summation of shifted, scaled and rotated cubic curves, each with a certain length $L$ and thickness $\tau$. If we consider just one of these curves (i.e. a single spaghetti) then the continuous definition of the image, assuming no shifting or rotation, is given by the following equation:

$$I(\mathrm{x}) = \left(1 - \frac{f(\mathrm{x})}{\tau^2}\right)\left(1 + \mathrm{e}^{(\mathrm{x}^{\mathrm{T}}\mathrm{x} - L^2)/(50\tau^2)}\right)^{-1} \mathrm{e}^{-f(\mathrm{x})/(2\tau^2)},$$

where $f(\mathrm{x}) = \left|y - a_1 x^3 - a_2 x\right|^2 / (1 + \left|3a_1 x^2 - a_2\right|^2)$. The coefficients $a_1$ and $a_2$ describe the cubic curve and $\mathrm{x} = [x, y]^{\mathrm{T}}$ is the continuous coordinates of the image. Note that re scale the coordinates such that $x, y \in [-1, 1]$. Using this equation, we can now easily generate rotated and shifted spaghetti by applying a rotational transformation with a translation to the coordinates $\mathrm{x}$.

To generate the images used in the paper, we created 25 individual spaghettis, each with randomly chosen coefficients, lengths, shifts and rotations. Note that the shifts were restricted such that spaghetti stayed within the range of the image. Using these parameters, the feature-full images were created by setting $\tau = 0.04$ and the feature-less were created by setting $\tau = 0.2$. Examples of both are shown in Fig. 1.

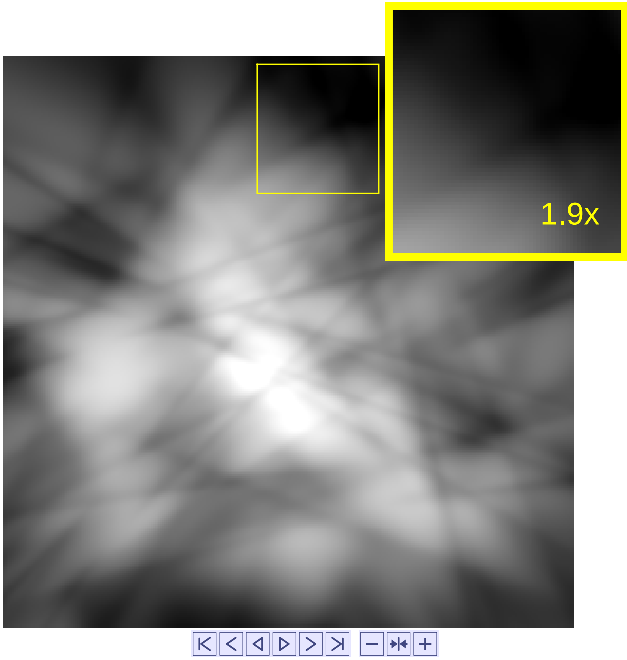


(a) Feature-less Images

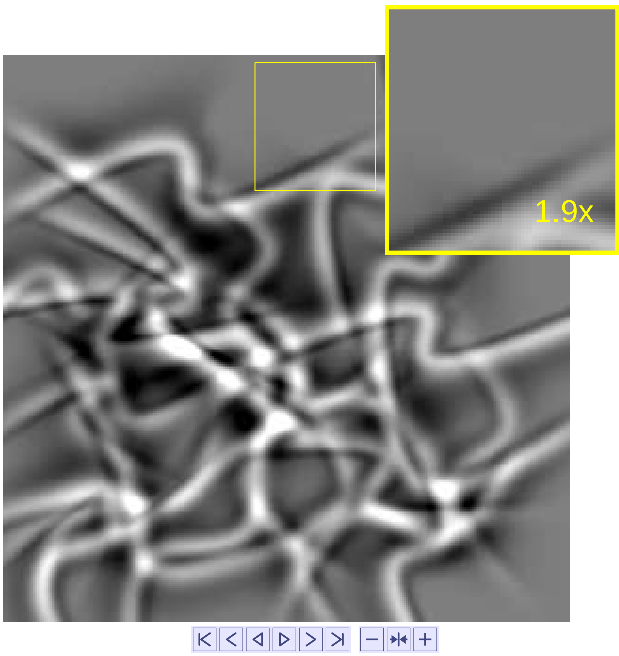


(b) Feature-Full Images

Fig. 1. Examples of the Feature-full and Feature less spaghetti images used in the main paper. Both images are subject to a quadratic deformation.

## II. Median and Median Absolute Errors for Section V-C

In this section, we show both graphs for the median and mean absolute deformations errors obtained by the algorithms when the input images are corrupted by Gaussian noise. The graphs are shown in Fig. 2.

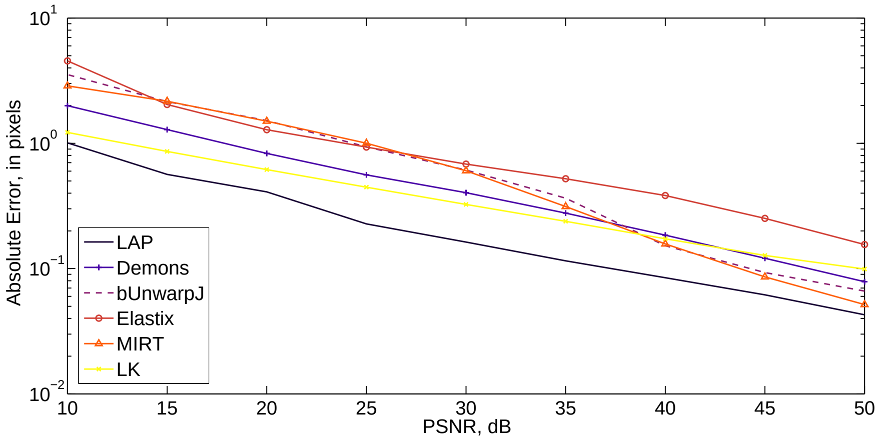


(a) Median Absolute Deformation Error, in pixels

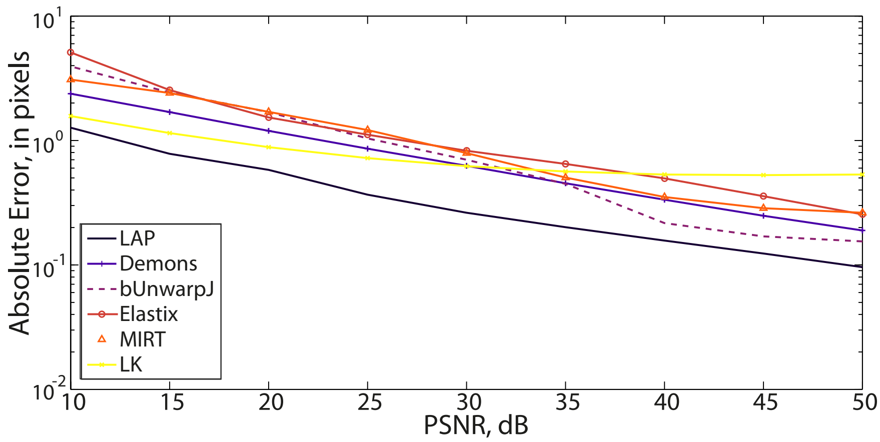


(b) Mean Absolute Deformation Error, in pixels

Fig. 2. Graphs showing the absolute deformation error for the PF-LAP and a selection of image registration algorithms obtained when the input images are corrupted by varying levels of additive white Gaussian noise. The median absolute error values are compared in (a) and the mean values in (b).

## III. Demonstration of the Registration Accuracy of the PF-LAP on the Oxford Affine Images

In this section, we provide an animation demonstrating the registration results obtained by the PF-LAP on the Oxford Affine Images.


(a) Original Images


(b) After Registration

Fig. 3. Animations showing the registration achieved by the PF-LAP when applied to the Bikes Images.


(a) Original Images


(b) After Registration

Fig. 4. Animations showing the registration achieved by the PF-LAP when applied to the Leuven Images.


(a) Original Images


(b) After Registration

Fig. 5. Animations showing the registration achieved by the PF-LAP when applied to the Wall Images.

## IV. Demonstration of the Registration Accuracy of the PF-LAP on the Retinal Images

In this section, we provide an animation demonstrating the registration results obtained by the PF-LAP on the Retinal Images. The animation of the images prior to registration are shown in Fig. 6a and after registration in Fig. 6b.

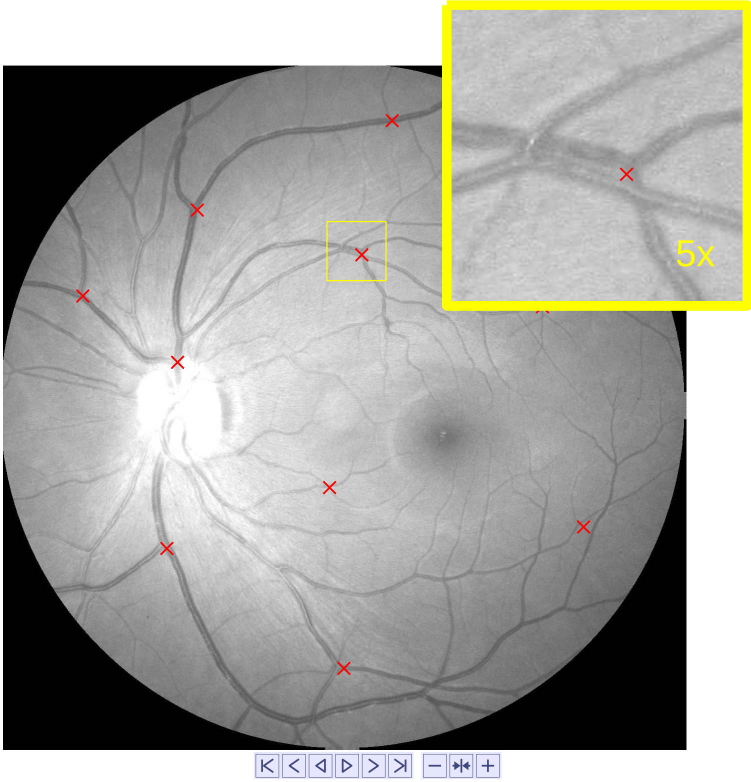


(a) Original Images

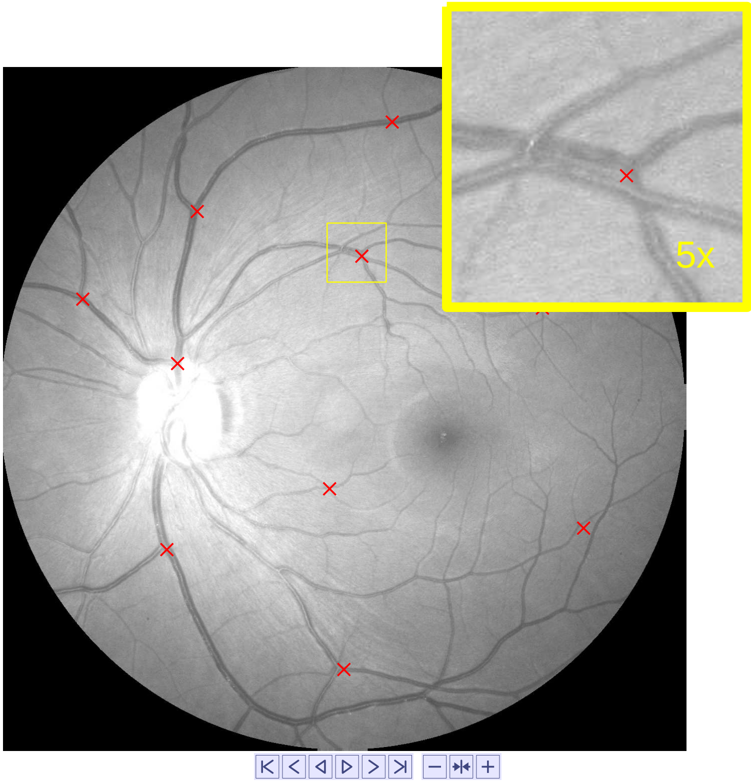


(b) After Registration

Fig. 6. Animations showing the registration achieved by the PF-LAP when applied to the Retinal Images.